

## A Deuterium NMR Study of Selectively Labeled Polybutadiene Star Polymers

C. H. Adams,<sup>‡,§</sup> M. G. Brereton,<sup>‡</sup> L. R. Hutchings,<sup>†</sup> P. G. Klein,<sup>\*,‡</sup> T. C. B. McLeish,<sup>‡</sup> R. W. Richards,<sup>†</sup> and M. E. Ries<sup>‡</sup>

*IRC in Polymer Science and Technology, University of Leeds, Leeds LS2 9JT, U.K., and University of Durham, Durham DH1 3LE, U.K.*

*Received May 17, 2000*

**ABSTRACT:** From a combination of tailored synthesis and deuterium NMR free induction decay (FID) measurements, the molecular dynamics of various entanglement sections in four-arm star polybutadienes has been studied. Each arm of the polybutadiene stars has a monodisperse molecular weight of 30 000 g mol<sup>-1</sup>, and each has a deuterated sequence of molecular weight 2000 g mol<sup>-1</sup>. This sequence, which corresponds to an entanglement length, has been located at different distances from each arm end, namely one entanglement length from the free end, 1/4, 1/2, and 3/4 of the way down the arm to the star core and at the core. Although the FIDs from the core and near the free end are always distinctly different, the FIDs from the other sections are only clearly distinguishable above ca. 40 °C. This is interpreted in terms of the molecular weight corresponding to the longest Rouse mode detectable on the NMR time scale at various temperatures. The deuterium FIDs have been analyzed according to an exact solution for the transverse relaxation, which produces an effective correlation time that increases toward the core of the star and with decreasing temperature.

### Introduction

Molecules of branched topology have a profound effect on the melt processing of polymers and hence are the subject<sup>1–3</sup> of extensive study. The simplest model of such a molecular architecture is the star polymer, where several polymer chains are connected to a common junction. There is currently much interest<sup>4–6</sup> in the tailored synthesis of model star polymers, whereby molecules of well-defined functionality and monodisperse arm length are produced, allowing the results of physical characterization studies to be sensibly interpreted within the context of theoretical dynamical models. In a previous paper,<sup>7</sup> details of the synthesis of a series of polybutadiene star polymers, of functionalities 3, 4, 8, and 12 were reported. Each star had a similar arm molecular weight of approximately 30 000 g mol<sup>-1</sup>. The dynamic rheology of these star polymers was interpreted using a model developed by Ball and McLeish,<sup>8</sup> which arises from considering the possible molecular mechanism by which stress relaxation can occur in a star polymer. In common with other theories,<sup>9</sup> this is essentially understood within the framework of the tube model but recognizes that reptation cannot occur in a star polymer because of the presence of the junction. Instead, relaxation is controlled by fluctuations of the entangled tube length, in which the free end of the star arm retraces some of its tube before a further outward exploration of the melt. This motion completely renews the configuration of the outer part of the arm as far as the deepest retraction. In consequence, each entanglement length of the star arm is considered to have its own characteristic correlation time, which, for the *relaxation of stress*, will increase exponentially<sup>8</sup> with distance from the free end. However, within the tube model, stress is essentially held by *tube segments* unvisited by a free chain end—it is this that is observed

by rheology. The reorientation of the actual chain segment within the tube will follow different dynamics. However, this basic idea, that there are a range of orientational correlation times, localized to entanglement sections, while intuitively reasonable, has not, to our knowledge, been directly observed experimentally, and it is a primary objective of the present paper to do so.

To this end, we have synthesized a family of 4-arm star polybutadienes, all of monodisperse arm molecular weights of around 30 000 g mol<sup>-1</sup>, with deuterated entanglement lengths situated at various distances from the free end of the star arm, in an otherwise fully hydrogenous polymer. The deuterium NMR transverse relaxation is therefore a direct experimental probe of the dynamics of specific entanglement sections. To interpret the results, we have employed, for the first time, an exact solution for the transverse relaxation time<sup>10</sup> incorporating a single orientational correlation time. We have recently used<sup>11</sup> similar deuterium NMR methodologies to quantify Rouse and reptation dynamics in linear polybutadiene chains of various molecular weight, and parameters calculated in that study will be used in the present work.

Selective labeling to isolate the dynamics of specific parts of a polymer chain has been used by others, particularly in the investigation of networks.<sup>12–14</sup> In most cases, the deuterated sequence was rather short, approximately 30 deuteriobutadiene monomers, and the networks were randomly cross-linked. Of particular relevance to the data we present here was the use of 4-arm star polybutadienes with the deuterated sequences at the junction and the free ends of each arm that were subsequently cross-linked. It was noted that the deuterium NMR spectrum for the free end had a broader line width than that for the junction, but no attempt was made to model these data. Deuterium NMR has also been applied to study chain dynamics in coronas of ionomer aggregates,<sup>15</sup> namely poly(styrene-*b*-sodium acrylate) reverse micelles and sodium car-

<sup>‡</sup> University of Leeds.

<sup>†</sup> University of Durham.

<sup>§</sup> Present address: Department of Chemistry, University of Sheffield, Sheffield S3 7HF, U.K.

boxylate terminated polystyrene aggregates. A sequence of three monomer units in the polystyrene chain were deuterated and located at various points along the chain. Deuterium line widths, signal intensities, and relaxation times were measured, and the local bond correlation times were calculated by means of the standard Bloch–Purcell–Pound theory. It was concluded that a molecular mobility of the ionic junction is dramatically reduced and that even at a distance of 25 repeat units from the nonionic block junctions, the mobility was still less than that in free chains.

In our previous paper which concentrated mainly on the rheology<sup>7</sup> of polybutadiene star polymers of various functionality, we showed a deuterium NMR spectrum of the free, end entanglement section of the arm. It had a Lorentzian line shape, which is consistent with this section of chain undergoing Rouse dynamics.<sup>16</sup> The end section is, therefore, undergoing entirely different dynamics than the other (approximately 14) entanglement sections along the arm, which can only reorient when the arm retracts the required distance along the tube confining it, as described above. In the present work, we therefore examine sections from the core through to the penultimate entanglement length only, to provide a self-consistent picture of the range of dynamics along the star arm.

## Experimental Section

**Synthesis of Labeled Star Polymers.** The entanglement molecular weight ( $M_e$ ) of polybutadiene, calculated from literature values<sup>17</sup> of the plateau modulus, is  $1\,970\text{ g mol}^{-1}$ . In this work, a series of four-arm polybutadiene star-branched polymers have been synthesized in which the target molecular weight of each arm was  $30\,000\text{ g mol}^{-1}$ , approximately 15 entanglement lengths. Each arm is labeled with a short section of polydeuteriobutadiene of molecular weight equivalent to approximately one entanglement length. The arms are, in effect, isotopic copolymers of butadiene and deuteriobutadiene. In all, six stars of this type have been prepared, in which the position of the labeled section varies from the very core of the star to the tip of each arm.

The precursor arm poly(butadiene–deuteriobutadiene) copolymers were prepared by the sequential addition of the monomers, using anionic polymerization and classic high-vacuum techniques. Benzene (distilled and dried over calcium hydride) was used as the solvent and *sec*-butyllithium (1.3 M solution in cyclohexane, Aldrich) as the initiator. Deuteriobutadiene was prepared by the reductive dechlorination of hexachlorobutadiene according to the procedure of Craig and Fowler.<sup>18</sup> Butadiene (Aldrich) was passed through a drying column prior to use. After the polymerization of each block, a sample of polymer was removed for molecular weight determination. From high-resolution, solution-state NMR measurements, the polymer microstructure was determined as 45% *cis* and 45% *trans* 1,4- and 10% 1,2-polybutadiene.

Construction of the star-branched polymers was achieved by adding sufficient silicon tetrachloride to the solution of living precursor arm polymer, to give a 25% mole excess of living polymer ends with respect to Si–Cl bonds. The mixture was stirred at 50 °C for 2 days to allow complete coupling before terminating the excess, unreacted living arm polymer with nitrogen sparged methanol. The product was collected by precipitation into methanol. The excess arm polymer was separated from the star-branched polymer by multiple fractionations, using toluene as the solvent and methanol as the nonsolvent.

Molecular weight determination was carried out by size exclusion chromatography (SEC), using both concentration and viscosity detectors. It has been shown that SEC elution volumes for star-branched polymers can show a marked dependence upon the solution concentration. As a result of this, the universal calibration method may yield molecular weight

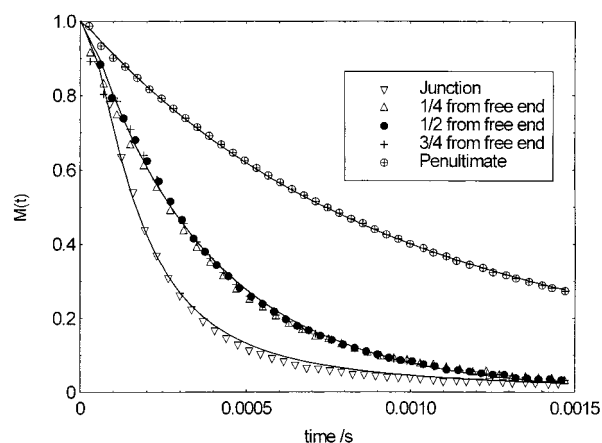


**Figure 1.** Deuterium transverse relaxations  $M(t)$  at 20 °C from the various labeled segments within the star arm. The solid lines are fits to data using eq 5. For clarity, not all data points are included.

**Table 1. Molecular Weight of the Deuteriobutadiene Block, Position of the Deuteriobutadiene Block, Molecular Weight of the Whole Arm Precursor, and Arm Polydispersity (Pd) Used in the Synthesis of Four-Arm Partially Deuterium-Labeled Polybutadiene Stars**

position of deuteriobutadiene block	$\bar{M}_w$ block	$\bar{M}_n$ block	$\bar{M}_w$ arm	$\bar{M}_n$ arm	Pd arm
core	1800	1800	36 900	37 000	1.00
$3/4$ from end <sup>a</sup>	2000	1700	30 100	29 900	1.01
$1/2$ <sup>b</sup>	2400	2200	33 300	32 300	1.03
$1/4$ from end <sup>c</sup>	3200	3100	33 000	33 000	1.00
penultimate <sup>d</sup>	2300	2300	24 800	24 800	1.00
end	2100	2100	29 800	29 800	1.00

<sup>a</sup> The exact position of the deuterated block begins at  $\bar{M}_w$  22 400 from tip. <sup>b</sup>  $\bar{M}_w$  16 100 from the tip. <sup>c</sup>  $\bar{M}_w$  8400 from the tip. <sup>d</sup>  $\bar{M}_w$  2000 from the tip.

**Table 2. Molecular Weight, Functionality, and Polydispersity (Pd) of Four-Arm, Partially Deuterium-Labeled Polybutadiene Stars**

position of deuteriobutadiene block	$\bar{M}_w$ star	$\bar{M}_n$ star	Pd	functionality
core	144 000	143 000	1.00	3.9
$3/4$ from end	122 200	115 100	1.06	4.0
$1/2$	132 400	132 400	1.00	4.0
$1/4$ from end	113 200	107 700	1.05	3.5
penultimate	93 200	91 100	1.02	3.8
end	111 000	111 000	1.00	3.7

values that are lower than the true values. However, we have ascertained that for stars in this molecular weight range no concentration dependence was evident.<sup>7</sup> Tables 1 and 2 provide details of the precise location and molecular weight of each deuterated entanglement section in the star arm, together with arm and star molecular weights, polydispersity indices, and functionalities.

**Nuclear Magnetic Resonance.** On-resonance free induction decay signals (FIDs) were recorded on a Chemagnetics CMX-200 spectrometer, operating at 30.7 MHz for deuterium. Standard single-pulse experiments were performed, typically using a 90° pulse width of 2.75  $\mu$ s, 1024 data points, 2  $\mu$ s dwell, recycle delay of 15 s, and 2048 acquisitions. All samples were degassed and sealed under vacuum prior to the NMR measurements.

## Results and Discussion

**General Features of the FIDs.** FIDs were measured at temperatures from –30 to +60 °C. Figure 1 shows the FID from each deuterated section, recorded at 20 °C. First, it is clear that the NMR is sensitive to the range of dynamics exhibited by the different en-

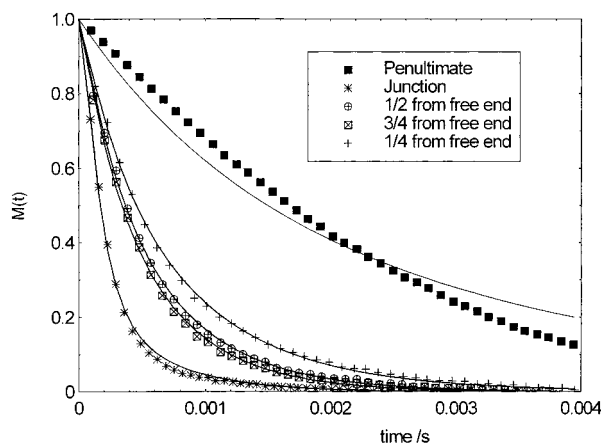


**Figure 2.** Deuterium transverse relaxations  $M(t)$  at 60 °C from the various labeled segments within the star arm. The solid lines are fits to data using eq 5. For clarity, not all data points are included.

tanglement sections. The FID from the penultimate section decays slowly, corresponding to relatively fast dynamics, consistent with this section being in close proximity to the free end of the arm. Conversely, the FID from the section situated at the core decays rapidly, corresponding to relatively slow dynamics, which is consistent with the constraint exerted by the tetrafunctional star junction. Second, the FIDs from the sections situated at fractional distances of  $1/4$ ,  $1/2$ , and  $3/4$  from the free end, while lying between the FIDs from the extremes, are nevertheless indistinguishable from each other, a result that is initially surprising.

Figure 2 shows the FIDs recorded at a higher temperature of 60 °C. There are two main differences between these data and those shown in Figure 1. First, the FIDs at the higher temperature do, in general, decay more slowly than at the lower temperature, indicating that raising the temperature reduces the orientational correlation time, as expected. Second, there is now a discrimination between the sections situated  $1/4$ ,  $1/2$ , and  $3/4$  from the free end. From hereon, these sections will be referred to as “removed from the extremes”, and we shall return to this point later.

It has been pointed out to us by a referee that, because the polymers are only partially deuterated, there is the possibility of some residual proton–deuterium dipolar interaction, which may not be fully averaged by molecular motion and could therefore contribute to the rate of decay of the FID. To check for this, the FIDs for some samples were recorded with high power (approximately 63 kHz) proton decoupling during the acquisition. The FIDs with and without the decoupling were identical, within experimental error, suggesting that the molecular motion effectively averages this dipolar interaction.

In Figure 3, we plot  $T_2^*$  (the time for the FID to decay by a factor of  $1/e$ ) versus temperature, from  $-30$  to  $+60$  °C. It should be emphasized at this point that none of the FIDs are single exponential (except perhaps that of the penultimate section), hence the required use of the exact solution<sup>10</sup> to be discussed, and so the NMR relaxation time  $T_2$  has little significance other than being a convenient indicator of the rate of decay of the transverse relaxation. For all the sections apart from the core,  $T_2^*$  increases with temperature, indicating the dynamics are approaching the extreme narrowing regime. This has also been confirmed from deuterium  $T_1$  measurements,<sup>19</sup> the  $T_1$  increasing from 9.5 ms at 20 °C to 24 ms at 60 °C. The  $T_1$ 's of the different sections

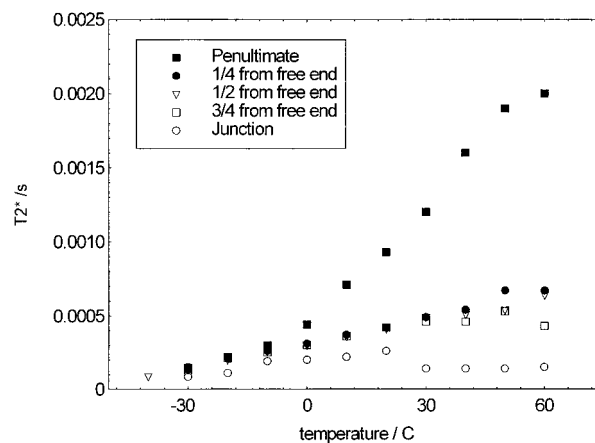


**Figure 3.** Transverse relaxation times  $T_2^*$  for the various labeled segments within the star arm as a function of temperature.

at any temperature are identical, within error, consistent with the  $T_1$  being sensitive only to the very local motions. The  $T_2^*$  of the core section is virtually insensitive to temperature, suggesting this section is strongly confined by the tetrafunctional junction and interchain entanglements, giving it dynamics similar to a chemically cross-linked network chain. The discrimination between the dynamics of the sections removed from the extremes is only revealed above about 40 °C.

**Difference between FIDs at 20 and 60 °C: A Quantitative Explanation.** We now return to the principal difference between the data in Figures 1 and 2—that the FIDs from the sections removed from the extremes are distinguishable at 60 °C but not at 20 °C. We explain this in terms of the Rouse relaxation times of the entanglement sections. We argue that, although the three deuterated sections removed from the extremes do not travel to the junction or free end of the molecule, there is an influence of these extremities on the dynamics of the midsections, which is revealed on the NMR time scale, at some temperature between 20 and 60 °C. It has been shown that, at short times, even entangled linear polymers lose orientational correlation first through short Rouse modes, and then progressively longer Rouse modes before arm-retraction or reptation mechanisms take place.<sup>7</sup> Here, we argue that, at the elevated temperatures, the deuterated sections  $1/4$  and  $3/4$  from the free end become aware of the free end and junction, respectively, through the long Rouse modes of the star arm.

The shortest Rouse mode that would be necessary for the section  $1/4$  from the end to be influenced by this free end is that corresponding to a section of chain of molecular weight  $M_a/4$ , where  $M_a$  is the molecular weight of one arm. Similarly, the Rouse mode that would be necessary for the section  $3/4$  from the end to be aware of the core is also that corresponding to a molecular weight of  $M_a/4$ , because this section is situated  $M_a/4$  from the core. The effect of the core on this section, however, would be to slow it down, compared to its dynamics in a linear chain of molecular weight  $M_a$ . Because the distance of the sections  $3/4$  and  $1/4$  are each the same distance from their nearest extremity, they would become aware of the presence of the extremity at the same time.

Let the Rouse time of a section of chain of molecular weight  $M_a/4$  be denoted as  $\tau_{1/4}$ . A test of the long Rouse mode hypothesis is whether the distinction between the various sections after a time equal to  $\tau_{1/4}$  will be



perceived within some typical time scale for the NMR experiment. An appropriate time to use as a measure of the duration of the NMR experiment is  $T_2^*$ . To demonstrate quantitative support for the hypothesis of Rouse modes, it is necessary to find the length of chain, in terms of molecular weight, which corresponds to the longest Rouse mode possible within time  $T_2^*$ . Rouse times are proportional to the square of molecular weight,<sup>20</sup> and so the Rouse time  $\tau'$  for a section of chain of molecular weight  $M$  is given by

$$\tau'(M) = \tau \left( \frac{M}{m} \right)^2 = T_2^* \quad (1)$$

where  $m$  and  $\tau$  are the molecular weight of the Rouse unit and its fundamental Rouse time, which have values of 260 g mol<sup>-1</sup>, and 8.3 × 10<sup>-7</sup> s, respectively.<sup>11</sup> From Figure 3, the  $T_2^*$  at 20 °C is approximately 0.4 ms. From eq 1 this gives a value for  $M$  of 5700 g mol<sup>-1</sup>.  $M_a$  for these samples is 30 000 g mol<sup>-1</sup>, and so the value for  $M$  corresponds to about  $1/5 M_a$ . This shows that at 20 °C, within the time scale of the NMR experiment, any given section can only perceive the effects of anything up to  $1/5 M_a$  away. This is slightly less than the  $1/4 M_a$  necessary for the section  $1/4$  or  $3/4$  from the free end to perceive the free end or the junction. This therefore provides an explanation for the overlapping FIDs from the sections removed from the extremes at 20 °C.

To perform the same calculation at 60 °C, we require the correlation time  $\tau$  for a Rouse unit at this temperature. Applying a simple WLF shift<sup>21</sup> from 20 to 60 °C leads to a predicted  $\tau$  of 1.5 × 10<sup>-7</sup> s at 60 °C. From Figure 3 it can be seen that the  $T_2^*$  for the sections removed from the extremes is about 0.6 ms. Equation 1 then leads to a molecular weight of 16 400 g mol<sup>-1</sup>, approximately half the length of the star arm. Therefore, it is quite reasonable to assume that at the elevated temperature, on the time scale of the NMR experiment, the  $1/4$  and  $3/4$  sections will execute dynamics influenced by the free end and the core of the star arm, respectively. Consequently, the three sections removed from the extremes can be discriminated in the FID at this temperature.

**Quantitative Analysis of the FIDs.** In this part of the paper, we shall fit the FIDs to a theoretical model, which allows calculation of a characteristic orientational correlation time, and this quantifies the range of dynamics exhibited by the different entanglement sections in the star arm. To analyze the FIDs, a theoretical result developed by Brereton<sup>10</sup> will be employed. This analytic result is an exact solution for the transverse NMR relaxation from a labeled statistical segment whose self-correlation function is that of a single exponential. This theoretical result  $G(t, \Delta, \tau_b)$  for the transverse relaxation signal from an NMR-active segment, whose dynamics is described by a single correlation time  $\tau_b$ , can be written as follows:

$$g(t, \Delta, \tau_b) = \sqrt{\frac{4K}{(1+K)^2 - (1-K)^2 \exp(-2tK/\tau_b)}} \exp\left(\frac{-t(K-1)}{2\tau_b}\right) \\ K \equiv K(\Delta, \tau_b) = \sqrt{1 + 2i\Delta\tau_b} \\ G(t, \Delta, \tau_b) = \text{Re}[g(t, 2\Delta, \tau_b) g(t, -\Delta, \tau_b) g(t, -\Delta, \tau_b)] \quad (2)$$

The theoretical signal is determined from two key

parameters:  $\Delta$ , the rescaled quadrupolar interaction strength, and  $\tau_b$ , the single correlation time. This model is valid for both fast ( $\Delta\tau_b \ll 1$ ) and slow dynamics ( $\Delta\tau_b \gg 1$ ), unlike the commonly employed second moments approximation, which is only valid for fast dynamics. In the limit of fast dynamics ( $\Delta\tau_b \ll 1$ ),  $K \approx 1$  in eq 2, leading to

$$G(t, \Delta, \tau_b) = \exp\left(-\frac{3}{2}\Delta^2\tau_b t\right) \quad (3)$$

which is the familiar single-exponential decay of transverse magnetization, where we can identify

$$\frac{3}{2}\Delta^2\tau_b = \frac{1}{T_2} \quad (4)$$

where  $T_2$  is the spin-spin relaxation time.

Any statistical segment in a polymer chain is known to display a wide spectrum<sup>10</sup> of correlation times, making the NMR determined  $\tau_b$  an *effective* correlation time. This  $\tau_b$  is determined by the type of polymer dynamics, for example Rouse or reptation. As will be seen, this approach generates extremely good fits, with correlation times that can usefully be understood in the light of previous work<sup>11</sup> on linear polybutadiene melts.

In our previous work<sup>11</sup> on linear polybutadiene melts it was necessary to introduce two rescaled quadrupolar interaction strengths, termed  $\Delta_1$  and  $\Delta_2$ . Computer simulation revealed that the fast local level atomic motion averaged the NMR interaction term differently for the methylene and methine deuterium nuclei. The short linear chains in the previous paper were analyzed using a result<sup>16</sup> for Rouse chains, with the interesting finding that only one friction coefficient was required. That is, despite the intrinsic differences in atomic level mobility, reflected by the two  $\Delta$  values, the longer time scale reorientations can be well described by a single representative chain, with one local friction coefficient corresponding to the length scale of the statistical unit. Therefore, in our model we are justified in using a single effective correlation time  $\tau_b$  even though there are two  $\Delta$  values.

The FIDs were analyzed using the function  $M(t, \tau_b)$  given by

$$M(t, \tau_b) = \frac{2}{3}G(t, \Delta_1, \tau_b) + \frac{1}{3}G(t, \Delta_2, \tau_b) \quad (5)$$

where the fractional contributions simply come from the proportions of methylene and methine deuterium nuclei in the butadiene repeat unit. The two  $\Delta$  values are taken from the work<sup>11</sup> on linear chains, which yielded  $\Delta_1 = 4600$  Hz and  $\Delta_2 = 7900$  Hz, leaving only one fitting parameter, the effective correlation time  $\tau_b$ . Each labeled section over the temperature range -30 to 60 °C has been fitted to eq 5. The value of  $\tau_b$  for each data set was determined by a least-squares approach and can be found in Table 3. Above -20 °C, this approach generates good fits as can be seen in Figures 1 and 2. When the effective correlation time  $\tau_b$  becomes too large, the theoretical function  $G(t, \Delta, \tau_b)$  becomes insensitive to this parameter. This happens<sup>10</sup> when  $\Delta\tau_b \geq 10$  and puts an upper limit on the value for  $\tau_b$  that can be reliably determined, as approximately 2 ms. Below -20 °C it is impossible to find a satisfactory fit using eq 5 without allowing  $\Delta_1$  and  $\Delta_2$  to increase in magnitude. Underlying the theory in eqs 2 and 5 is the assumption of relatively

**Table 3. Correlation Time  $\tau_b$  ( $\mu$ s) for Each Deuterated Section at Various Temperatures ( $^{\circ}$ C), from Fits to Eq 2**

temp	core	$3/4$	$1/2$	$1/4$	penultimate
60	>2000	61.7	47.3	35.8	11.5
50	335	64.6	54.1	42.7	11.9
40	1360	71.4	62.4	52.4	15.8
30	>2000	78.7	69.0	63.6	19.1
20	>2000	90.7	89.6	81.7	24.1
10	>2000	134	117	117	36.3
0	>2000	224	179	205	61.1
-10	>2000	1050	579	1080	127
-20	>2000	>2000	>2000	>2000	1620
-30	>2000	>2000	>2000	>2000	>2000

fast local level dynamics. At these lower temperatures, this assumption is no longer valid. From inspection of Table 3 it can be seen that, in general, the values for  $\tau_b$  follow a logical trend in that  $\tau_b$  becomes shorter at higher temperature and also toward the free end of the star arm. However, the variation of  $\tau_b$  with location of the entanglement section has nothing like the exponential dependence predicted<sup>8</sup> from theories quantifying the rheology, as discussed in the Introduction. This would appear, at first sight, to be a severe discrepancy, but we should recognize that the molecular processes required for relaxation of stress are entirely different from those required for the decay of transverse nuclear magnetization. In the former case, the characteristic time is that required for the reorientation of the *tube* segments,<sup>8</sup> which involves diffusion of the free end of the star arm, within the tube, to the segment under consideration. The deuterium NMR transverse relaxation, however, arises from reorientation of the chain segments themselves. Within the context of the tube model, we may consider this to occur via curvilinear Rouse motion within the unmodified tube segment, which will clearly occur on a much shorter time scale than stress relaxation.

It is interesting to compare the effective correlation times found from the analysis of the star samples at 20  $^{\circ}$ C with our earlier work<sup>11</sup> on linear polybutadiene also at 20  $^{\circ}$ C. For simplicity, but without loss of generality, we will only consider the signal arising from the methylene deuterium nuclei. The penultimate section to the free end of the star arm is not very constrained by the entanglement structure in the melt. It is therefore anticipated that the FID will be similar to that of a free chain of a molecular weight equal to the entanglement molecular weight.<sup>22</sup> Such a chain generates a transverse relaxation signal given by<sup>11</sup>

$$G_{\text{Rouse}}(t) = \exp\left(-\frac{6}{\pi}\Delta_1^2\tau\ln N_e t\right) \quad (6)$$

where  $\tau$  is the shortest Rouse time and  $N_e$  is the number of Rouse units in an entanglement length, that is

$$N_e = \frac{M_e}{m} \quad (7)$$

where  $M_e$  is the entanglement molecular weight and  $m$  the molecular weight of a Rouse unit.<sup>11</sup> At 20  $^{\circ}$ C the penultimate section has parameters (Table 3) such that  $\Delta_1\tau_b = 0.1$ , making eq 2 a valid approximation. For our single correlation time result (eq 3) to correspond to the Rouse result (eq 6) requires the effective correlation time  $\tau_b$  to be written as

$$\tau_b = \frac{4\ln N_e}{\pi}\tau \quad (8)$$

The entanglement molecular weight  $M_e$  is approximately 2000 g mol<sup>-1</sup>, and from our previous work,<sup>11</sup> we obtained a value of 260 g mol<sup>-1</sup> for  $m$  and  $8.3 \times 10^{-7}$  s for  $\tau$ , leading to a value for  $N_e$  of 7.7 and a predicted  $\tau_b = 2.2 \times 10^{-6}$  s. The fit of eq 5 to the FID obtained from the penultimate section from the free end gave a value of the effective correlation time,  $\tau_b$ , of  $2.4 \times 10^{-5}$  s (Table 3). That the effective correlation time for this penultimate section is larger than that of the Rouse chain prediction might be expected. The penultimate section has an entanglement length of chain attached to one end and the rest of the star arm to the other. It is therefore not unreasonable that the effective correlation time is somewhat larger than that anticipated by the free Rouse chain comparison. This determined effective correlation time therefore compares favorably with our earlier work<sup>11</sup> on linear polybutadiene.

Next we consider the data obtained from the section  $1/2$  of the way from the end. This will be compared to the predicted correlation time from a reptating linear chain of the same molecular weight to that of the star arm. From this we can evaluate the influence of attaching one end of the chain to the star core and assess how sensitive NMR is to this constraint. A reptating chain is predicted<sup>22</sup> to generate a transverse relaxation as follows:

$$G_{\text{reptation}}(t) = \exp\left[-\frac{18}{\pi}\Delta_1^2\tau\frac{M}{M_e}\ln\left(\frac{M}{M_e}\right)t\right] \quad (9)$$

For the section  $1/2$  way from the end, we find (Table 3) that  $\Delta_1\tau_b = 0.4$ . This is not truly within the fast dynamics limit, necessitating the use of the exact solution (eqs 2 and 5) and is borne out by the fact that the FID of this section is not a single exponential. However, for the purpose of the comparison, we are attempting to make between star and linear polymer dynamics, it is convenient to use the fast dynamics approximation of eq 3, especially as the FID only departs significantly from a single exponential at times longer than  $T_2^*$ . For our single correlation time result eq 3 to correspond to the reptation result eq 9 implies

$$\tau_b = \frac{12}{\pi}\frac{M}{M_e}\ln\frac{M}{M_e}\tau \quad (10)$$

Here,  $M$  is taken to be the molecular weight of a star arm (30 000 g mol<sup>-1</sup>), leading to a predicted  $\tau_b = 1.3 \times 10^{-4}$  s. The fit of eq 4 to data obtained from the section  $1/2$  way from the end yields a value of  $\tau_b$  of  $9.0 \times 10^{-5}$ , which is remarkably close to this anticipated value. This reveals that, over the time scale that this NMR experiment is sensitive, the section  $1/2$  way from the end of the star arm is behaving similarly to that of the midsection of a corresponding linear reptating chain.

For the core section the effective correlation time  $\tau_b$  was generally found to be at least  $2.0 \times 10^{-3}$  s. This can be seen to be reasonable by considering that the correlation time increases by a factor of 4 on going from the penultimate section to the  $1/2$  section. It is therefore not surprising that there is at least another order of magnitude increase as the labeling moves from the midsection to the core, giving a minimum expected value of  $10^{-3}$  s.

## Conclusions

We have shown how deuterium NMR of selectively labeled star polymers can quantify the range of correlation times exhibited by different entanglement sections along the star arm. The FIDs have been interpreted according to an exact solution<sup>10</sup> for the transverse relaxation, which yields an effective orientational correlation time  $\tau_b$  for each section. At constant temperature,  $\tau_b$  increases from the free end of the star arm toward the star core. In general,  $\tau_b$  for any specific section increases with decreasing temperature, although the assumptions inherent in the model put an upper limit of about 2 ms on the reliable determination of  $\tau_b$ . An interesting result of the analysis is that NMR appears to be insensitive to the difference between the dynamics of the central section of a star polymer and that of an analogous section in a linear polymer of molecular weight equivalent to the star arm. This is essentially because relaxation of transverse magnetization occurs within a few milliseconds, during which time the distinctly different dynamics exhibited by star polymers and linear polymers, which would contribute, for example, to stress relaxation, will not be apparent.

The FIDs from the central sections (those situated at fractional distances of  $1/4$ ,  $1/2$ , and  $3/4$  along the arm) were found to be identical at room temperature but distinguishable at higher temperatures. An explanation for this result was found from consideration of the molecular weight corresponding to the longest Rouse mode possible within the NMR time scale. At room temperature, this molecular weight corresponded to only about one-fifth of the arm length, leading to the conclusion that the dynamics of the central sections would not be influenced by the extremities. At 60 °C, this increased to one-half the arm length; hence, it was reasonable to assume that the sections situated fractional distances of  $1/4$  and  $3/4$  from the end would be influenced by the rigid core and flexible free end, leading to faster and slower decays, respectively.

**Acknowledgment.** Financial support from EPSRC to the IRC in Polymer Science and Technology, the research program of which this study forms a part, and

the provision of a maintenance grant to C.H.A. are gratefully acknowledged. We are indebted to Professor P. McDonald and Dr. M. A. N. Driver for discussions concerning measurement of transverse relaxation and to Mr. G. P. Hughes for carrying out complementary deuterium  $T_1$  measurements.

## References and Notes

- (1) McLeish, T. C. B.; Milner, S. T. *Adv. Polym. Sci.* **1999**, *143*, 195.
- (2) McLeish, T. C. B. *Curr. Opin. Solid State Mater. Sci.* **1997**, *2*, 678.
- (3) Bishko, G.; McLeish, T. C. B.; Harlen, O. G.; Larson, R. G. *Phys. Rev. Lett.* **1997**, *79*, 2352.
- (4) Huckstadt, H.; Gopfert, A.; Abetz, V. *Macromol. Chem. Phys.* **2000**, *201*, 296.
- (5) Pitsikalis, M.; Sioula, S.; Pispas, S.; Hadjichristidis, N.; Cook, D. C.; Li, J. B.; Mays, J. W. *J. Polym. Sci., Part A: Polym. Chem.* **1999**, *37*, 4337.
- (6) Mah, S.; Hwang, H. S.; Shin, J. S. *J. Appl. Polym. Sci.* **1999**, *74*, 2637.
- (7) Adams, C. H.; Hutchings, L. R.; Klein, P. G.; McLeish, T. C. B.; Richards, R. W. *Macromolecules* **1996**, *29*, 5717.
- (8) Ball, R. C.; McLeish, T. C. B. *Macromolecules* **1989**, *22*, 1911.
- (9) Pearson, D. S.; Helfand, E. *Macromolecules* **1984**, *17*, 888.
- (10) Brereton, M. G. *J. Chem. Phys.* **1991**, *94*, 2136.
- (11) Klein, P. G.; Adams, C. H.; Brereton, M. G.; Ries, M. E.; Nicholson, T. M.; Hutchings, L. R.; Richards, R. W. *Macromolecules* **1998**, *31*, 8871.
- (12) Gronski, W.; Emeis, D.; Brüderton, A.; Maldaner-Jacobi, M.; Stadler, R.; Eisenbach, C. *Br. Polym. J.* **1985**, *17*, 103.
- (13) Gronski, W.; Stadler, R.; Moldaner-Jacobi, M. *Macromolecules* **1984**, *17*, 741.
- (14) Simon, G.; Baumann, K.; Gronski, W. *Macromolecules* **1992**, *25*, 3.
- (15) Gao, Z. S.; Zhong, X. F.; Eisenberg, A. *Macromolecules* **1994**, *27*, 794.
- (16) Brereton, M. G. *Macromolecules* **1989**, *22*, 3667.
- (17) Fetters, L. J.; Lohse, D. J.; Richter, D.; Witten, T. A.; Zirkel, A. *Macromolecules* **1994**, *27*, 4639.
- (18) Craig, D.; Fowler, R. B. *J. Org. Chem.* **1961**, *26*, 713.
- (19) Hughes, G. P., unpublished work, University of Leeds.
- (20) Doi, M.; Edwards, S. F. *The Theory of Polymer Dynamics*; Clarendon Press: Oxford, 1986.
- (21) Ferry, J. D. *Viscoelastic Properties of Polymers*; Wiley: New York, 1980.
- (22) Ries, M. E.; Brereton, M. G.; Klein, P. G.; Dounis, P. *Polym. Gels Networks* **1997**, *5*, 285.

MA0008490